Implication of a power-law power-spectrum for self-affinity

N. P. Greis*
Kenan-Flagler School of Business, CB No. 3490, Carroll Hall, University of North Carolina at Chapel Hill, Chapel Hill, North Carolina 27599-3490

H. S. Greenside†
Department of Computer Science and Department of Physics, Duke University, Durham, North Carolina 27706
(Received 30 April 1990; revised manuscript received 13 March 1991)

We examine numerically the self-affine scaling of time series with an imposed power-law power spectrum $P(\omega)=C\omega^{-\alpha}$, for different exponents $1\leq\alpha\leq 3$, and for different sequences of phases. We use two different criteria for testing self-affinity, a fractal dimension of the graph of the time series, and a more sensitive test based on the scaling of moments of probability distributions. For $\alpha\neq 2$, our results suggest that time series with a power-law spectrum are only approximately self-affine, even in the best case of long-time series with high-dimensional, δ-function-correlated, uniformly distributed phases. Scaling curves are most sensitive to phases with long correlation times, are weakly dependent on the shape of the phase probability distribution, and are independent of the fractal dimension of the phases.

I. INTRODUCTION

In several physical [1–4] and economic [5,6] examples, random times series have been found that have an approximate power-law power spectrum of the form

$$P(\omega)=C\omega^{-\alpha}\ , \tag{1}$$

where C is a positive constant and the exponent α is greater than or equal to 1. These time series are quite interesting, since they have no characteristic time scale and their correlation times [7] are comparable to the duration of the entire time series. Physical mechanisms for producing such time series are poorly understood except in the cases of Brownian motion ($\alpha=2$) and of white noise ($\alpha=0$).

Mandelbrot has suggested that time series with a power-law spectrum may be *self-affine* [8,9]. This is a particular kind of statistical self-similarity that implies the absence of characteristic time scales by assuming structure on all time scales. Mathematically, a time series $x(t)$ is self-affine if its increments

$$\Delta x(\tau)=x(t+\tau)-x(t) \tag{2}$$

for times t and time intervals τ satisfy the relation

$$\Delta x(\lambda\tau)=\lambda^{H}\Delta x(\tau)\ , \tag{3}$$

where equality between random variables means that they have identical probability distributions. The Wiener process, a mathematical model of Brownian motion with $H=\frac{1}{2}$, demonstrates that this definition is not an empty one [8]. The exponent H, which lies between 0 and 1, is called a Hurst exponent [8], Hölder exponent [10], or simply the scaling exponent in different contexts. Self-affine time series can then be classified by the parameter H. Positive identification of self-affinity and the exponent H in empirical time series would be a useful first step in modeling them [11,12,3].

A simple corollary [13] of Eq. (3) is that a self-affine times series $x(t)$ must have a power-law spectrum with exponent $\alpha=2H+1$. This raises the important converse question of whether the observed time series with power-law spectra are self-affine. This question has been partially addressed in recent years by several researchers [14–17], who have studied numerically some properties of time series with an imposed power-law power spectrum and with uniformly distributed phases. According to certain specific tests for self-affinity (discussed below in Sec. II C) these researchers found that time series were approximately self-affine for different values of the exponent α, although certain systematic errors occur. Higuchi [17] also found that if the range of the phases did not span the full interval $[0,2\pi]$, then there were significant deviations from self-affinity, e.g., a length-based fractal dimension had the wrong value. This implies that a power-law spectrum is *not* sufficient for a time series to be self-affine. This is not too surprising, since the power spectrum gives knowledge of just one moment out of an infinity of moments of the distributions in Eq. (3).

In this paper, we examine more carefully the self-affine properties of time series with power-law power spectra. Our goal is to determine more quantitatively when such time series are self-affine, so that empirical data can be better analyzed. We address this question numerically by investigating time series with imposed power-law spectra for different sequences of phases, in which we vary their probability distribution, their correlation time, and their fractal dimension. We find that tests of self-affinity based on fractal dimensions [1,16,17] are weakly dependent on the dimensionality and on the probability distribution of the phases, but deviate strongly from self-affinity if the correlation time is long. A more careful and direct test of self-affine scaling, based on studying average moments of Eq. (3), reveals a further dependence on the probability distribution (whether it is uniform or not), but not on the fractal dimension. In particular, nonuniformly distribut-

ed phases give poor scaling.

Our results concerning self-affinity are useful in several ways. First, the scaling curves and relative errors given below illustrate the quality of conclusions that may be deduced in an ideal case of a long-time series (of order a million points) and a known power spectrum. Second, our results clarify when the traditional random-phase approximation for random time series [18] is appropriate for modeling self-affine time series. Such times series are generally not Gaussian (although their increments may be) and do not obey a central limit theorem. It is not obvious that a statistical limit exists that is independent of the statistical properties of the phases. Third, our calculations give an interesting result, that the fractal dimension of time series with a power-law spectrum is empirically independent of the dimensionality of the phases used to generate those time series. We do not know of other cases where an *algebraic* transformation of a sequence changes the fractal dimension of that sequence.

The rest of the paper is as follows. In Sec. II, we discuss details of how we generate time series with a power-law spectrum with different phase distributions. We then discuss different numerical tests for self-affinity and explain the two methods that we use. In Sec. III, we present and discuss scaling curves for time series of roughly 1 000 000 points, varying the exponent α in Eq. (1) and varying the phase distributions. We also summarize various systematic errors in the scaling curves. Finally, in Sec. IV, we summarize our results.

II. METHODS

A. Generating the time series

In this section, we discuss how to generate time series with power-law power spectra and with different phase distributions. Following an approach used by many authors [14,19,15–17], we use discrete Fourier transforms to construct time series at evenly spaced points in time with a specified power spectrum. Other nonspectral algorithms have been discussed elsewhere [9,19] but these either have extra numerical parameters, complicating their analysis, or do not allow an easy variation of phases. It would be interesting at a later date, however, to reproduce some of our results with these other algorithms.

In our simulations, we calculate M values of a periodic time series $x(t)$ at equally spaced intervals of time $t_i = i\Delta t$, spanning a total period of time $T = M\Delta t$. For a fixed constant C and exponent α, the power spectrum Eq. (1) is imposed through the following equation [16]:

$$x_i = x(t_i) = \sum_{k=1}^{M/2} \sqrt{P(\omega_k)\Delta\omega}\cos(\omega_k t_i + \phi_k) \quad \text{for } 1 \le i \le M , \qquad (4)$$

where the frequencies $\omega_k = k\Delta\omega$ are multiples of the smallest discrete frequency $\Delta\omega = 2\pi/T$. The $M/2$ phases, $\phi_k \in [0, 2\pi]$, are the only source of fluctuations. Different realizations of the phases give different realizations of the time series.

Using Eq. (4), we typically generate a matrix of $N = 10$ realizations, x_i^μ, for $1 \le \mu \le N$ and $1 \le i \le M$, and then study various statistical properties of this matrix. The M sums in Eq. (4) are evaluated using a fast Fourier transform to avoid the expensive $O(M^2)$ operation count of direct evaluation. In this paper, all time series have length $M = 2^{17} = 131\,072$, so the effective total length of the time series (including realizations) is typically about 1 000 000. This is larger than nearly all time series used in physical and economic applications, although not long enough to study certain statistical limits. Convergence studies for longer series are difficult, since few computers have more than a few megawords of memory.

Although the power spectrum Eq. (1) has two parameters, one would expect that only the exponent α, and not the overall magnitude C, should be important in tests of self-affinity. An overall scaling of the power spectrum simply multiplies the corresponding time series by a constant, which should not affect its statistical properties. Surprisingly, the numerical studies of Fox [15], especially Fig. 7 of his paper, shows that this deduction is empirically incorrect. We do not understand this result, although we would guess that it is a consequence of the finite precision of computer arithmetic. In what follows, we fix $C = 1$ for all the time series, and vary α over the range [1,3].

B. The phase distributions

In this section, we discuss the different choices of phase distributions that are used in Eq. (4) to generate different kinds of time series with power-law spectra. In most references to date, researchers have used a random-phase approximation that was motivated by the classical Fourier analysis of random signals [18]. This approximation corresponds to using a high-dimensional, uniformly distributed, δ-function-correlated sequence of phases in the interval $[0,2\pi]$. This choice is suspicious in view of the now widespread knowledge that randomness in the form of low-dimensional chaos can arise from deterministic nonlinear equations with few degrees of freedom [20]. In particular, since fractal dimensions are often used to characterize self-affine time series, one should be concerned that the fractal dimension of the phases used in Eq. (4) may play a role.

To explore the effect of different phase distributions that might arise through nonlinear dynamics, we studied six different methods of generating sequences of phases, varying the probability distribution, the correlation time, and the fractal dimension. We did not examine further the result of Higuchi [17], who showed that a restricted range of the phases produced non-self-affine time series; all our distributions span the interval $[0,2\pi]$.

Our first choice of phases was a sequence that should approximate the random-phase approximation. We used the C-programmed function ran1 of Press *et al.* [21] to generate high-dimensional, uniformly distributed, approximately δ-function-correlated numbers x_k in the interval (0,1), We independently tested the dimensionality of output from ran1 using the Grassberger-Procaccia algorithm for the correlation dimension [22,23]. This test failed to show any finite-dimensional scaling of the out-

put from ran1 for time series with 2^{19} points, and for embedding dimensions up to 12. This is consistent with the assumption of a high-dimensional sequence, but the actual fractal dimension of ran1 is not known. The phases used in Eq. (4) were then defined by

$$\phi_k = 2\pi x_k \ . \tag{5}$$

Using these phases, we were able to reproduce selected results of Higuchi [17] and of Osborne and Provenzale [16] to a relative accuracy of a few percent.

A second choice was a sequence of low-dimensional and nonuniformly distributed numbers. We defined the phases ϕ_k to be $2\pi y_k$, where the one-dimensional sequence $y_k \in (0,1)$ was generated by iterating the logistic map

$$y_{i+1} = 4y_i(1-y_i) \ . \tag{6}$$

This chaotic sequence y_k is known analytically [24] to have the probability distribution $1/[\pi\sqrt{y(1-y)}]$, which is highly nonuniform and favors values near $y=0$ and near $y=1$. Different realizations of phases were determined by choosing different initial states $y_0 \in (0,1)$ and by iterating Eq. (6) $M/2$ times. We used the ran1 function to choose the different initial values y_0.

A third choice of phases was a low-dimensional but uniformly distributed sequence of numbers. Starting from a random initial condition $y_0 \in (0,2\pi)$, we iterated the logistic map Eq. (6) to produce a sequence y_k. We then transformed this sequence as follows:

$$\phi_k = 4 \arcsin(\sqrt{y_k}) \ . \tag{7}$$

These phases can be shown to be uniformly distributed in the interval $(0,2\pi)$ and to have dimension $D=1$.

For our fourth choice, we explored whether a continuous distribution of phases was significant. We chose the phases randomly from a *discrete* set of K equally separated values in the interval $[0,2\pi]$. Since several preliminary tests for self-affinity were observed to be only weakly dependent on the integer K for $K>2$, we set $K=3$ and chose phases randomly from the three values

$$\phi_k \in \{0, 2\pi/3, 4\pi/3\} \ , \tag{8}$$

according to whether the output from the ran1 function lay within the intervals $[0,\frac{1}{3})$, $[\frac{1}{3},\frac{2}{3})$, or $[\frac{2}{3},1)$, respectively.

Fifth, we chose phases from a continuous but asymmetric distribution

$$P(\phi) = \frac{1}{2\pi^2}(2\pi - \phi) \ , \quad \phi \in [0,2\pi] \tag{9}$$

that decreases linearly from a finite value at $\phi=0$ to zero at $\phi=2\pi$. This choice complements Eqs. (6) and (7) by testing the effects of a continuous, high-dimensional but nonuniform sequence of phases. Random variates obeying this distribution are given by the formula

$$\phi = 2\pi(1-\sqrt{1-x}) \ , \tag{10}$$

where x is a uniformly distributed random variate in (0,1).

Sixth, and finally, we studied whether rapidly decaying correlations in the phases were important, since all the above sequences of phases are approximately δ-function correlated. We generated nonperiodic phases with infinitely long-lived correlations using the quasiperiodic sequence

$$\phi_k = s_0 + \pi[\sin(k) + \sin(\sqrt{k})] \pmod{2\pi} \ , \tag{11}$$

which densely fills out the interval $[0,2\pi]$. Different realizations were determined by choosing different random shifts $s_0 \in (0,2\pi)$.

Figure 1 gives a feeling for how these different phase distributions affect the time dynamics of Eqs. (1) and (4) for the exponent $\alpha=2$. Figure 1(a) is the case corresponding to the random-phase approximation used by most researchers. Figure 1(b) is a time series whose phases are based on the logistic map, Eq. (6). The plot is qualitatively different in that local fluctuations are sub-

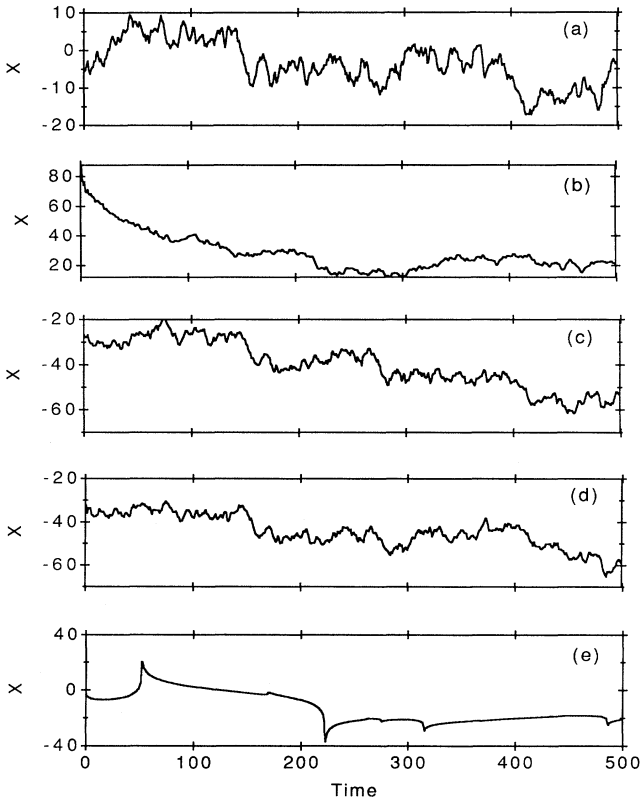

FIG. 1. Time series with a power-law spectrum, Eq. (1), for time step $\Delta t=1$, exponent $\alpha=2$, and for different phase distributions. The first 500 points are shown from much longer time series of length $M=131\,072$. (a) Uniformly distributed, high-dimensional phases from Eq. (5). (b) Nonuniformly, distributed, low-dimensional phases obtained by iterating the logistic map, Eq. (6). Essentially identical results are obtained for phases generated by Eq. (7). (c) Phases chosen randomly and uniformly from a discrete set of $K=3$ phases, Eq. (8). (d) Phases chosen from a high-dimensional, linearly decreasing probability distribution, Eq. (10). (e) Phases chosen from the quasiperiodic sequence, Eq. (11).

stantially smaller than those observed for uniformly distributed phases. Low-dimensional but uniformly distributed phases based on Eq. (7) give a plot that looks the same as Fig. 1(b) and is not shown. Plots of time series based on a discrete phase distribution, Fig. 1(c), and on an asymmetric linear distribution, Fig. 1(d), are qualitatively similar to Fig. 1(a). Quasiperiodic phases give the time series in Fig. 1(e), a smooth evolution interrupted irregularly by cusps. This time series is quite different from all time series generated with approximately δ-function-correlated phases.

This comparison of time series already suggests two useful qualitative observations. First, time series based on Eq. (4) are sensitive to the choice of phases, as already pointed out by Higuchi in a different context [17]. Second, the duration of temporal correlations seems to produce the strongest changes in the time series; the continuity of the probability distribution or the shape of the probability distributions is less important. These observations are confirmed in the more quantitative analysis given in Sec. III below.

It is also instructive to compare these $1/\omega^2$ time series with some familiar and closely related stochastic time series. Figure 2(a) is a realization of the Wiener process

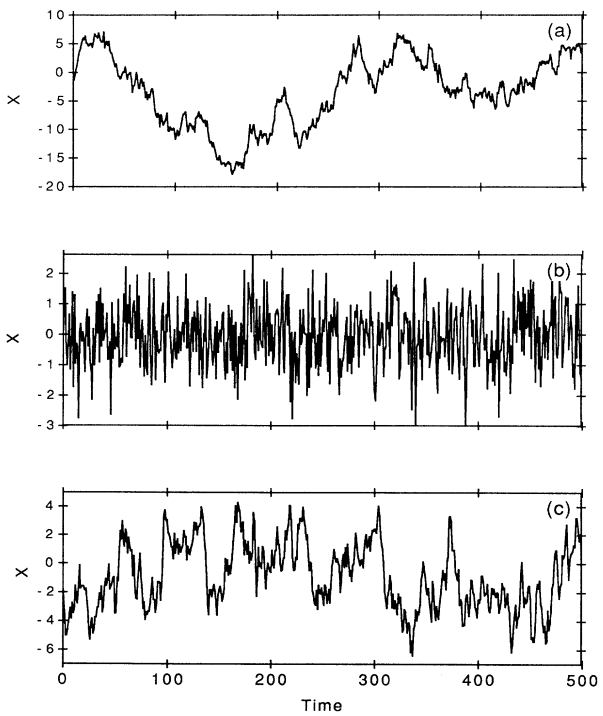

FIG. 2. First 500 points of realizations of three stochastic time series. (a) The self-affine Wiener process, approximated by iterating Eq. (12). The continuous path limit is self-affine and has a power-law spectrum with $\alpha=2$. (b) Gaussian noise of mean 0 and variance 1, obtained from the function gasdev [21]. (c) Realization of the Ornstein-Uhlenbeck process Eq. (13), with damping $\tau=1$, time step $\Delta t=1$, and noise strength $\xi=1$. The realization was calculated by numerical integration [37] using the initial condition $x_0=0$.

(Brownian motion), which can be approximated at constant time intervals Δt by iterating the difference equation

$$x_{i+1}=x_i+\sqrt{\Delta t}\,g_i \ . \tag{12}$$

The numbers g_i are drawn from a normal distribution. In the limit $\Delta t\to 0$, the Wiener process is known analytically to be self-affine [10] with a $1/\omega^2$ power spectrum, whereas no corresponding analytical results are yet known for Eq. (4). The qualitative similarity of Fig. 2(a) with Figs. 1(a), 1(c), and 1(d) suggests that Eq. (4) does approximate a self-affine series for $\alpha=2$ and for certain phase distributions. In contrast, time series based on Gaussian white noise, Fig. 2(b), or on the Ornstein-Uhlenbeck process Fig. 2(c), do not have a power-law power spectrum, and look qualitatively different. The Ornstein-Uhlenbeck process $x(t)$ satisfies the stochastic differential equation [25]

$$\frac{dx}{dt}=-\frac{1}{\tau_c}x+g(t) \ , \tag{13}$$

where $\tau_c>0$ is a constant characteristic time and $g(t)$ is δ-function-correlated Gaussian white noise of strength ξ, whose correlation function is given by

$$\langle g(t_1)g(t_2)\rangle=\xi\delta(t_1-t_2) \ . \tag{14}$$

Correlations decay exponentially with the characteristic time τ. One can also show that $x(t)$ has a power spectrum $P(\omega)\propto 1/(1+\tau^2\omega^2)$, which asymptotically approaches a power law only for large frequencies $\omega\gg 1/\tau_c$.

C. Diagnostics for self-affinity

In this section we discuss methods for testing self-affinity in time series. Since the definition, Eq. (3), involves equality of probability distributions, there is an infinity of testable conditions. This implies that one cannot establish self-affinity rigorously with a finite amount of data; one can only indicate that a time series is self-affine to some approximation for a certain class of tests. Our results are based on two criteria, a length-based fractal dimension [17], D, and an analysis of moments of Eq. (3) [see Eq. (17) below].

There are now many different methods for identifying self-affinity in time series. We briefly review them to give a sense of where our two tests fit in. We have already mentioned one, that the power spectrum is a power law, with the exponent α satisfying

$$\alpha=2H+1 \ , \tag{15}$$

where H is the scaling exponent in Eq. (3). This test is an empty one in what follows, since we are constructing the time series to have this property. We also do not discuss long-lived correlations between increments [9]. Although these correlations are a dramatic prediction for self-affine time series, we report results elsewhere that show that numerical tests of long-lived correlations have large fluctuations around their expected value, and are less useful for quantitative work.

Several related tests arise from the nonstationarity of

self-affine time series. Thus the variance of increments [9] $V(\tau)$ scales as τ^{2H}; the roughness of the time series [3] $w(\tau)$ scales as τ^{H}; and the rescaled range [9] R/S scales as $(\tau/2)^{H}$. The variable τ has two different meanings in these tests. In the first case, it represents a time interval separating two points in time. In the second and third cases, $\tau < T$ represents the length of a time interval $[0,\tau]$ contained in the entire observation time $[0,T]$ over which various averages are performed.

Other related tests arise from fractal aspects of self-affine time series. The path of a self-affine time series in N-dimensional Euclidean space is fractal [10], with Hausdorff dimension $D = \min(1/H, N)$. This fact was used by Osborne and Provenzale [16] in their study of correlation dimensions of time series with power-law spectra. The graph of a self-affine time series has a fractal dimension [8, 26],

$$D = 2 - H = \frac{5-\alpha}{2} , \tag{16}$$

with the obvious restriction $1 \le D \le 2$, since a two-dimensional plot lies in the plane. This test was used by Burlaga and Klein [1] and by Higuchi [17]. Finally, the zero set of a self-affine time series is fractal with Hausdorff dimension [27] $D = 1 - H$. To our knowledge, this test has not yet been applied to data.

Two final tests deal with the definition Eq. (3) more directly. This equation predicts that the probability distributions of scaled time increments $\tau^{-H}\Delta x(\tau)$ should be identical for all time intervals τ, i.e., empirical histograms of increments for different τ should all collapse onto a single curve [3]. One drawback of this diagnostic is that it is somewhat difficult to quantify the disagreement between different probability distributions. Also, the curve is insensitive to possible characteristic time scales.

These difficulties can be partially remedied by studying moments of Eq. (3), which is an additional test that we propose. Equation (3) implies the following relation:

$$S(\lambda,\beta) = \langle |\Delta x(\lambda\tau)|^{\beta} \rangle^{1/\beta} = \lambda^{H} \langle |\Delta x(\tau)|^{\beta} \rangle^{1/\beta} , \tag{17}$$

i.e., the quantity $S(\lambda,\beta)$ is proportional to the quantity λ^{H} for arbitrary positive numbers β. (Angular brackets again represent averages over time and over realizations.) The case $\beta = 1$ was studied by Osborne and Provenzale [16]. Given Eq. (17), one can test for self-affinity by plotting $\log(S)$ versus $\log(\lambda)$ for many values of β. The linear parts of the plots (if they exist) should all have the same slope H. Unlike the test for agreement of scaled probability distributions, Eq. (17) is sensitive to the time scales appearing in the problem, as we show in the next section.

We note that there has not yet been a careful quantitative or statistical analysis of the best way to establish self-affinity for a finite amount of data, nor has there been a systematic comparison of these different methods. A recent exception was an experimental study of particle transport by capillary waves [3], in which the collapse of probability distributions to a single curve, the roughness of time series, the variance of time series, and long-lived correlations of increments were studied side by side. However, these empirical results are difficult to interpret in the absence of control tests on known self-affine data of similar length.

For the results presented in the next section, we restricted ourselves to two tests of self-affinity. First, we used the averages of moments, Eq. (17), which we found to be one of the more sensitive and insightful tests. Second, we used a length-based dimension D suggested by Higuchi [14,17] to estimate the fractal dimension of the graph of the time series. Higuchi's algorithm estimates D by calculating an average total length in the one-norm $\langle L(\tau) \rangle$ of all points on the graph that are separated in time by the interval τ. This average length should then scale as $L(\tau) \propto \tau^{-D}$ for self-affine curves. We chose this method over others because it was easy to compute, and because we could compare our calculations more readily with Higuchi's earlier results. We do not claim that either of the two methods is optimal either statistically or computationally.

A serious difficulty in applying these two methods (and, in fact, in applying most of the above methods) is the need to identify scaling regimes on log-log plots and to determine corresponding scaling exponents. This is most commonly done by plotting the logarithm of some quantity (e.g., for the dimension D, we plot the quantity $\log[\langle L(\tau) \rangle]$ versus the logarithm of some independent variable [here $\log(\tau)$]. Theoretically, one should obtain a straight line for all values τ. Empirically, one rarely sees this behavior, as emphasized by Fox [15]. There is considerable ambiguity in identifying when and where a scaling law holds.

To identify more clearly where scaling regimes occur, we plot the local slope of the log-log plot versus the logarithm of the independent variable. This local slope should be a horizontal straight line where a power-law relation holds, and is visually superior to log-log plots in evaluating the range of a scaling regime. We illustrate this for estimating D in Fig. 3. The log-log plots in part (a) look reasonably linear to the eye, but the local-slope plots in part (b) show systematic errors; the local slope is not constant, but monotonically changes over most of the range in time. Only the data for $\alpha = 2$ give a good scaling regime, with an average value equal to the expected theoretical value of $D = 1.5$.

These and other plots reported below were made by evaluating the various statistics for about 40 values of τ that were geometrically spaced between the smallest and largest time intervals; this gives equally spaced points on the log-log plots. Local slopes were obtained by simple finite differences of nearest pairs of points. We found this to be a fairly good estimator of the local slope, e.g., smoothing the plot with moving averages or with least-squares fitting a spline did not give substantially better or worse results.

We conclude this section with a technical comment concerning the use of correlation dimensions [28] to study the dimension of paths of self-affine time series. Osborne and Provenzale [16] attracted considerable interest when they observed that a *stochastic* time series, generated using Eqs. (1) and (4) and the random-phase approximation Eq. (5), could have a *finite* correlation dimension. Unlike the capacity, Hausdorff, and other geometric dimensions [10], the correlation dimension is

based on invariant measures of bounded finite-dimensional deterministic flows [29]. For such flows, the correlation dimension gives a useful measure of their complexity as the approximate minimum number of independent modes needed to generate the observed time series.

Unfortunately, correlation dimensions cannot be meaningfully calculated for time series with power-law spectra. Such time series are nonstationary (e.g., variances increase with time) and produce unbounded paths in phase space, so that orbits recur (if at all) only finitely many times. This implies that invariant measures do not exist and that the formal mathematical limit for the correlation dimension [22]

$$\lim_{\epsilon \to 0} \lim_{N \to \infty} \log[C(N,\epsilon)]/\log(\epsilon) \tag{18}$$

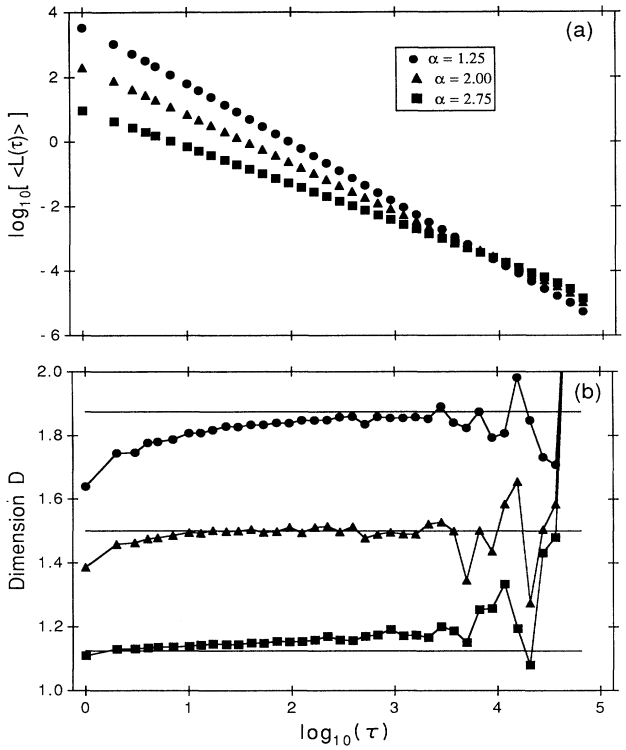

FIG. 3. Illustration of the advantages of plotting the local slope (b) of a scaling relation, compared to a direct log-log plot (a). The results are for the length-based dimension D proposed by Higuchi [14]. Time series of length $M = 131\,072$ were calculated with power-law spectra for exponents $\alpha = 1.25$, 2.0, and 2.75 using the random-phase approximation Eq. (5). Part (a) shows the log-log plot of the average length in the one norm, $\langle L(\tau) \rangle$, of the graph of the time series for points separated in time by τ. This gives three approximately straight lines. Part (b) shows the corresponding local slopes as estimated by finite differences between neighboring points. The three horizontal lines indicate the exact answers—$D = 1.875$, 1.5, and 1.125, respectively—predicted by Eq. (16). The average values of the local slope over the central two-thirds give the empirical values $D = 1.85$, 1.50, and 1.16, respectively, which have errors of order a few percent.

does not exist. Here $C(N,\epsilon)$ is the average number of pairs of N points in phase space that are closer than ϵ in some norm. The points in phase space are obtained by embedding the time series directly with time delays [22] or by using realizations as different coordinates [16].

For nonstationary time series, the correlation dimension determines the scaling only of points in phase space that are close in time, rather than between recurring points that are far apart in time. The scaling information is now similar to the Hausdorff dimension or length-based dimensions, and cannot be interpreted as an estimate of dynamical complexity. Given this fact, there is little motivation to use a correlation dimension for nonstationary time series with long correlation times, since it is much more expensive to compute [23] ($O[M \log(M)]$ instead of $O(M)$ operations for graph-based dimensions) and much less accurate for scaling exponents $H \ll 1$, the case of high-dimensional paths. It might be more fruitful to calculate the correlation dimension of increments instead, since these are often more stationary than the original time series.

This point has been made especially clearly by Theiler [30], who has recommended that correlation dimension algorithms discard pairs of points that are closer in time than about the correlation time. For approximately self-affine time series, whose correlation times are comparable to the length of the entire series, most points are discarded and the calculation cannot be completed. Further difficulties in estimating correlation dimensions of nonstationary time series have been discussed by Theiler elsewhere [31]. There he analytically determines the various scaling regimes of the correlation dimension for time series with Gaussian increments as a function of the length of the time series and as a function of low- and high-frequency cutoffs to a power-law power spectrum. He finds that all finite-dimensional scaling regimes are artifacts arising from the finite length of the time series.

III. RESULTS AND DISCUSSION

A. Length-based dimension

We begin by discussing the results of analyzing the length-based dimension D for time series with power-law spectra, and with different phase distributions. Figure 4 summarizes the scaling curves for the case $\alpha = 2$, which turns out to be fairly representative of other curves obtained for different values of α, with $1 < \alpha < 3$. Figure 4(a) was obtained by using the random-phase approximation Eq. (5). There is fairly accurate scaling over most of the time range, with significant deviations only occurring at very short times ($\tau < 10$) and at very long times ($\tau > 3500$). Deviations at the longest times τ are expected in all cases because the averages used to obtain the average length $\langle L(\tau) \rangle$ become noisier and noisier, with fewer and fewer terms included as τ approaches half the length of the time series.

Figure 4(b) is the case of uniformly distributed low-dimensional ($D = 1$) phases. The scaling curve is essentially identical to the high-dimensional case, suggesting that length-based dimensions are not sensitive to the

dimensionality of the phase distribution. Figure 4(c) is a control test, obtained by analyzing an approximation to the Wiener process, Eq. (12). This curve indicates accurate scaling down to the smallest time scales, which is substantially different from curves (a) and (b). At the longest time scales, the same curve shows somewhat larger fluctuations compared to (a) and (b), but we are not sure if this is a significant effect. Figure 4(d) was obtained from Eq. (4) for quasiperiodic phases, Eq. (11). There is now a clear absence of scaling; the local slope smoothly increases about 1.1 to about 1.7 over the entire time interval. The average value of the local slope is substantially smaller than the expected theoretical value of $D=1.5$ for $\alpha=2$. From this and other curves corresponding to other values of α (not shown), we deduce that long-lived correlations in the phases do not lead to self-affine scaling, even when a power-law power spectrum is imposed.

Because of the short- and long-time-scale errors suggested by Fig. 4, we estimate numerical values of the dimension D' by averaging the local slope only over the middle range $0.3\times5\leq\log_{10}(\tau)\leq0.7\times5$. This typically gives values that differ by about 10% from values obtained by using the entire range of data.

We summarize the results of many calculations similar to Fig. 4 in Fig. 5. This plot gives the relative error $(D'-D)/D$ between the numerically estimated dimension D' and the analytical dimension that is predicted for truly self-affine time series, given by Eq. (16). The relative error is plotted as a function of the exponent α for each of the phase distributions discussed in Sec. II B. For phases that are approximately δ-function correlated, the relative errors are nearly identical, as indicated by the top five curves in the plot. This suggests that length-based fractal dimensions are insensitive to the probability distribution (continuous, discrete, uniform, or nonuniform) or its fractal dimension (1 or ∞). As already pointed out in our discussion of Fig. 4(d), one obtains poor scaling for phases with long correlation times. Nevertheless, we have plotted the relative error for this case, estimating the dimension D' by an average over all time intervals τ. The relative error is now quite large (the curve labeled by circles in Fig. 5) and is suggestive of what may be observed for other non-self-affine time series.

We have repeated many of these calculations using the correlation dimension [22] of paths of realizations in sufficiently high-dimensional phase spaces. The relative error between the empirical correlation dimension ν' and the predicted correlation dimension $\nu=\min(1/H,N)$ is qualitatively similar to Fig. 5, although with much larger error bars. In particular, the correlation dimension is also weakly dependent on all details of the phases except for their correlation time. This is consistent with our discussion at the end of Sec. II C, where we pointed out that the correlation dimension effectively reduces to a geometric dimension for dynamics that lack a bounded invariant measure.

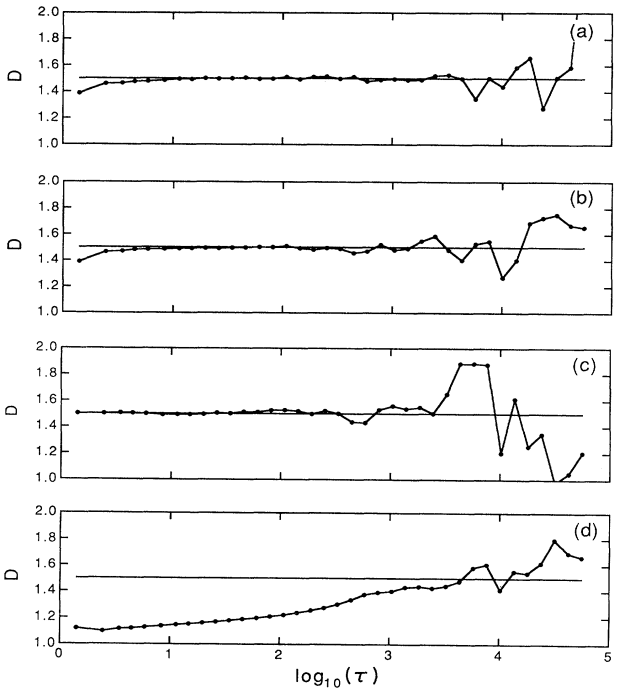

FIG. 4. Local slopes of scaling plots for the length-based dimension [17] obtained from time series of length $M=131\,072$ points and time steps $\Delta t=1$. (a) Power-law spectrum with $\alpha=2$ and high-dimensional uniformly distributed phases, Eq. (5). (b) Power-law spectrum with $\alpha=2$ and low-dimensional uniformly distributed phases, Eq. (7); an identical curve is obtained for the nonuniformly distributed phases, Eq. (6). (c) Realization of the Wiener process. (d) Power-law spectrum with $\alpha=2$ and quasiperiodic phases, Eq. (11).

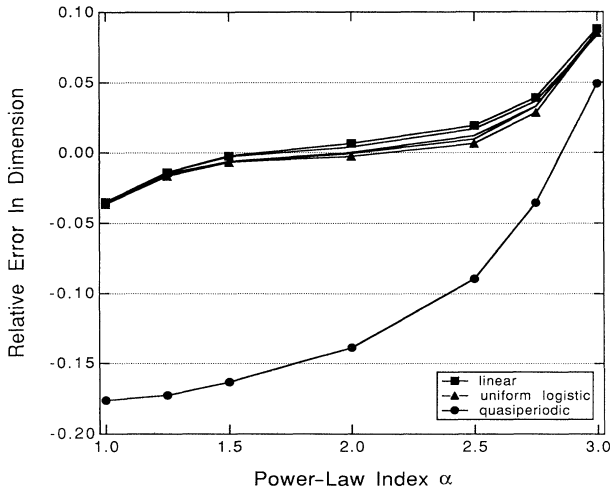

FIG. 5. Plot of relative errors in the dimension D vs the power-law exponent α, for the six choices of phase distributions of Sec. II B. All data were based on time series of length $M=131\,072$ and were generated with Eq. (4). For approximately δ-function-correlated phases (the top five curves), the relative error is of order 10% and is approximately symmetric around $\alpha=2$. Time series generated with quasiperiodic phases gave poor scaling results, with large systematic errors (the lowest curve).

B. Moments of probability distributions

We now turn to a discussion of results of analyzing moments, Eq. (17), for time series with power-law power spectra, and with different phase distributions. We first study thoroughly the scaling curves for $1/\omega^2$ spectra in Figs. 6 and 7, since Wiener noise provides an important and independent control test. Later figures then show illustrative results for other values of α in Fig. 8, and show how the relative error in the scaling exponent H varies with the exponent α, Fig. 9.

In these figures, scaling regimes and exponents are identified by plotting the local slopes of $\log[S(\tau,\beta)]$ versus $\log(\tau)$ [see Eq. (17)] for the first five integer moments, $\beta=1$ through $\beta=5$. For self-affine time series, these slopes should be independent of both β and of τ, giving the same value H, the scaling exponent in Eq. (3). Further, this average value H should be related to the exponent α of the power-law power spectrum through Eq. (15), i.e., $H=(\alpha-1)/2$.

As a useful control test, we first studied numerical Wiener noise, Eq. (12), which should approximate a true self-affine series with $H=\frac{1}{2}$. We see in Fig. 6(a) that the five different moments collapse onto the correct constant value $H=\frac{1}{2}$ for moderate times ($\tau<100$), but start to oscillate and separate for longer times, of order half the length of the entire time series. This behavior is quite similar to the corresponding dimension-based local-slope curve in Fig. 4(c). The numerical algorithm Eq. (12) evidently does not capture the longer time-scale structure of Wiener noise correctly.

Figure 6(b) gives the corresponding local-slope curves for time series with a prescribed $1/\omega^2$ spectrum in the random-phase approximation, Eq. (5). The self-affine scaling is not as satisfactory at small time scales when compared to Wiener noise, but is substantially improved at the longer time scales. For the case $\alpha=2$, we conclude that Eq. (4) with phases Eq. (5) produces a good approximation to a self-affine curve. This, unfortunately, does not remain the case for other values of α, especially for values near $\alpha=1$ or $\alpha=3$, as shown later in Fig. 8.

Figure 6(c) corresponds to low-dimensional nonuniformly distributed phases, obtained by iterating the logistic map, Eq. (6). Unlike the corresponding dimension plot Fig. 4(b), we now see strong evidence of non-self-affine scaling. The local slopes for higher moments are

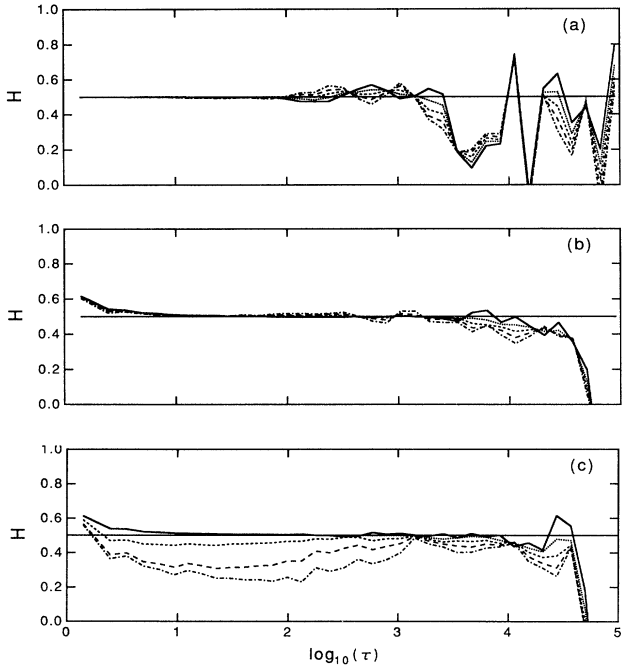

FIG. 6. Plots of the local slope of scaling curves obtained from Eq. (17) for the first five integer moments $\beta=1-5$. For self-affine time series, these slopes should all have the same constant value H. In each panel, the solid curve is $\beta=1$ and the straight horizontal line is the theoretical value $H=\frac{1}{2}$ for $\alpha=2$. These curves were calculated for time series with power-law power spectra with exponent $\alpha=2$, of length 131 072, for different phase distributions. The averages in Eq. (17) were carried out over time and over ten realizations. (a) Wiener process, Eq. (12). (b) High-dimensional, uniformly distributed phases, Eq. (5). (c) Low-dimensional ($D=1$), nonuniformly distributed phases, Eq. (6).

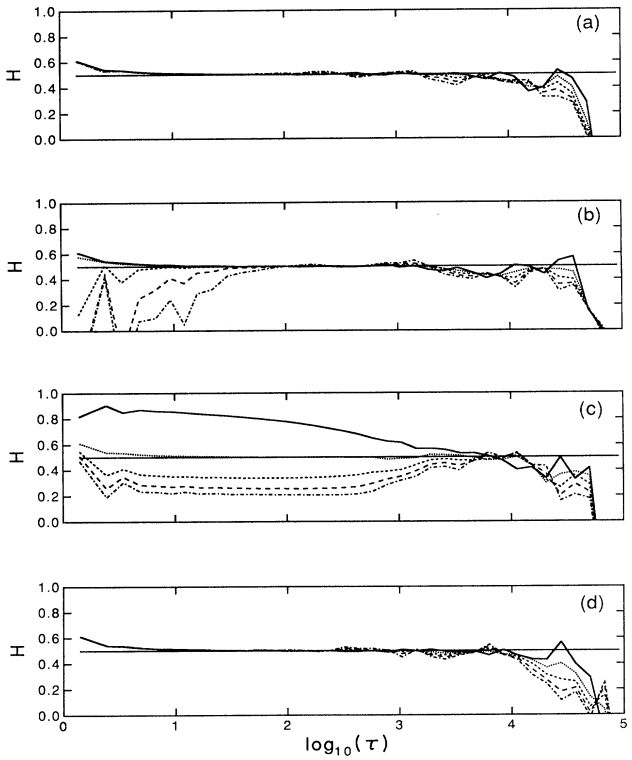

FIG. 7. Continuation of Fig. 6, showing the local slopes of Eq. (17) for time series with $\alpha=2$ and different phase distributions. (a) Discrete uniform phase distribution, Eq. (8). (b) Linearly distributed high-dimensional phases, Eq. (9). (c) Quasi-periodic phases, Eq. (11). (d) Uniformly distributed low-dimensional ($D=1$) phases, Eq. (7).

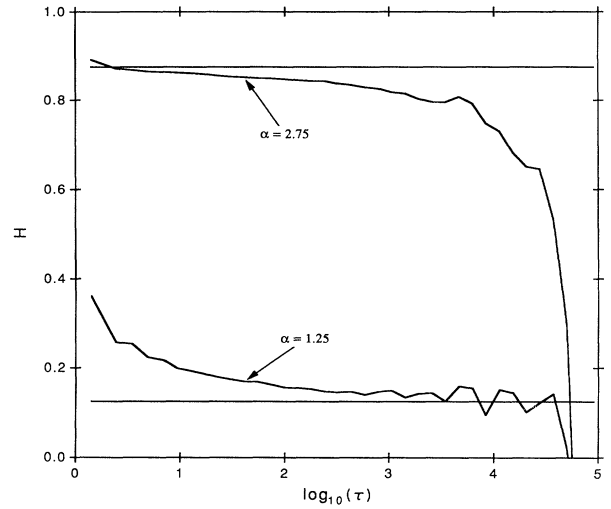

FIG. 8. Local slopes of scaling curves for Eq. (17) for $\alpha=2.75$ and $\alpha=1.25$. We show only the $\beta=1$ curves and only the best case of the random-phase approximation, Eq. (5). The horizontal straight lines are the expected theoretical values predicted by Eq. (15), $H=0.88$ and 0.125, respectively. There are substantial and systematic deviations from scaling.

approximately constant, suggesting the existence of scaling regimes, but they differ substantially from the expected value of $H=\frac{1}{2}$, decreasing for larger values of β. The $\beta=1$ curve consistently gives the best estimates of the scaling exponent H for different values of β and of α. We conclude that the scaling of moments of Eq. (3) is a more subtle test of self-affinity than fractal dimensions, since the latter cannot distinguish between the phase distributions Eqs. (5), (6), and (7) (Fig. 5).

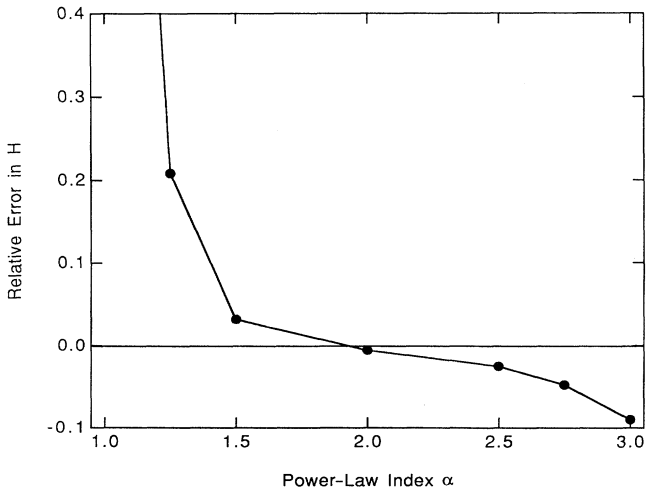

FIG. 9. Relative error ($\Delta H/H$) in the scaling exponent H of Eq. (17) as determined for $\beta=1$ and for high-dimensional uniformly distributed phases. The relative error diverges as $\alpha\rightarrow 1$ since H goes to zero in that limit, magnifying small errors.

Scaling curves for $\alpha=2$ and the other phase distributions discussed in Sec. II B are shown in Fig. 7. These curves, together with those in Fig. 6, can be summarized as follows. For the case $\alpha=2$, fairly accurate approximations to self-affine time series are obtained for phase distributions that are uniformly distributed and δ-function correlated. It does not matter if the phase distribution is discrete [Fig. 7(a)] or if the fractal dimension of the phases is small [Fig. 7(d)]. Nonuniformly distributed phases [Figs. 6(c) and 7(b)] produce non-self-affine scaling, although this is not picked up in dimension tests. The worst approximations for self-affine time series arise from phases with long correlation times, Fig. 7(c).

The situation for power-law exponents α with values other than 2 is less satisfactory. Figures 3 and 8 both suggest that Eqs. (1) and (4) with the random-phase approximation are poor approximations to self-affine time series when α becomes close to 1 or 3. In both these plots, the local slope increases slowly and monotonically, so that a good scaling region does not exist. It is difficult to say whether these are good or bad self-affine approximations without further comparisons to data that are more accurately self-affine.

The relative error in the empirical estimate of the scaling exponent H is shown in Fig. 9 for different values of α, for the case $\beta=1$, and only for time series generated in the random-phase approximation. This plot says that scaling exponents can be estimated to about 10% accuracy for most values of α between 1 and 3; this ignores the complexity that good scaling regimes are actually not found, as previously observed. The relative error is smallest near $\alpha=2$ and varies smoothly from positive to negative values as α is increased through that value. These results are similar to those of Fig. 5 and provide further support for the observation that time series with a power-law spectrum are approximately self-affine only for $\alpha\approx 2$.

Our conclusions are similar to, but more extensive than, conclusions already made by Osborne and Provenzale [16] and by Higuchi [17], who already observed systematic errors in the correlation dimension and length-based dimensions of time series with power-law spectra. These authors did not study, however, the possible more-general dependence on different kinds of phases.

We have not investigated the question of how the relative errors in these figures may decrease for even longer time series. The amount of data we have used—ten realizations of 131 072 points each—is already much larger than that used in many experiments or in economic databases. Higuchi [17] has studied how the dimension D depends on the length of the time series over the range 2^{14} to 2^{19}. He found very slow convergence of D towards the expected values of $D=2$ and $D=1$ for $\alpha=1$ and $\alpha=3$, respectively. We have confirmed this slow convergence, which has discouraged us from pursuing this question of convergence numerically.

C. Time series with characteristic times

We conclude this section on results by discussing briefly the possible self-affine scaling properties of the

Ornstein-Uhlenbeck process, Eq. (13), for which there is a characteristic time scale in the correlation function. The power spectrum of this process is asymptotically a power-law ($1/\omega^2$) for large frequencies $\omega \gg 1/\tau_c$. High-frequency power-law behavior in power spectra is, in fact, a general property of noisy flows and of some experimental data [32,33]. Such behavior cannot occur for chaotic solutions of finite-dimensional smooth bounded flows. In this case, power spectra decay exponentially for sufficiently high frequencies [34]. Crossover regimes for deterministic equations have been observed from power-law to exponential decay [35], which complicates the identification of stochastic systems with asymptotic power laws in the spectrum.

The question then arises whether the high-frequency part of the Ornstein-Uhlenbeck process is approximately self-affine when this power-law regime is attained. Figure 10 shows the local slopes for dimension and self-affine scaling tests for the Ornstein-Uhlenbeck process in (a) and (b), respectively. Both curves indicate a crossover regime, from approximately self-affine scaling with $D=1.5$ and $H=\frac{1}{2}$ at small time scales, to non-self-affine scaling for larger times. The values $D=2$ and $H=0$ are typical

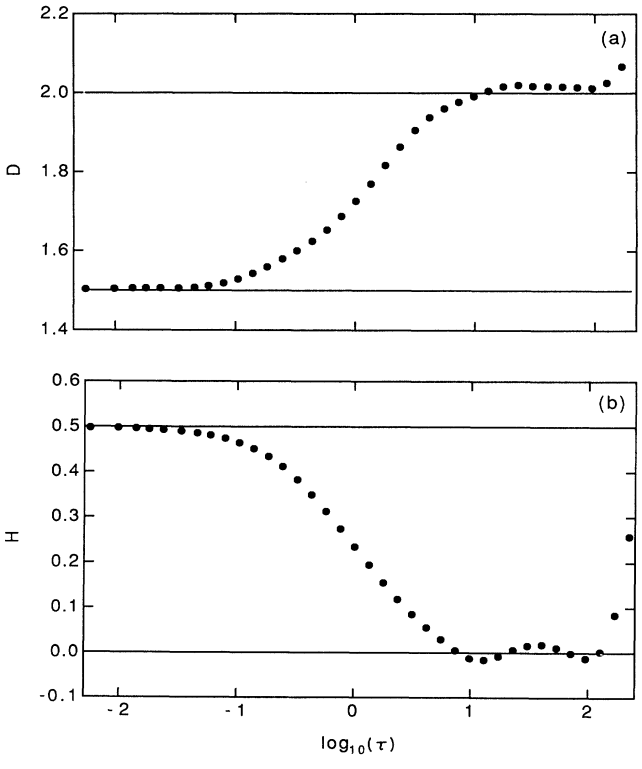

FIG. 10. Local slope of scaling curves for Higuchi dimension, part (a), and $\beta=1$ moment of Eq. (17), part (b), for ten 131 072-point realizations of the Ornstein-Uhlenbeck process, Eq. (13). The time series were calculated by numerical integration [37] with step size $\Delta t=0.004$, damping $\tau=1$, and noise strength $\xi=1$. The local slopes have been smoothed with a three-point moving average to remove high-frequency ripple.

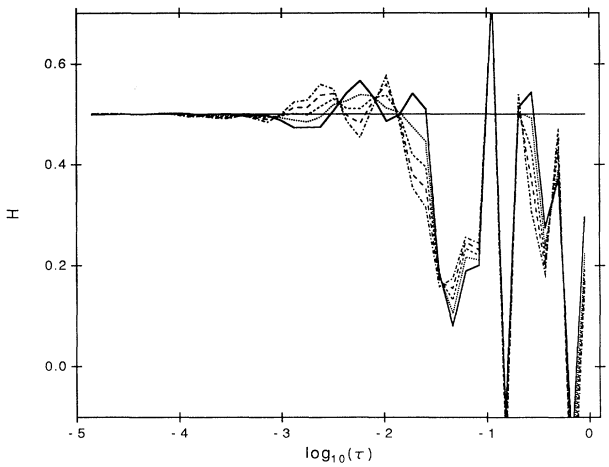

FIG. 11. Local slope of scaling curves for $\beta=1-5$, obtained from Eq. (17) for the Ornstein-Uhlenbeck process. The same parameters are used as given in Fig. 10, except a much smaller time step of $\Delta t=10^{-5}$ was used.

of high-dimensional white noise, which is what would be expected for times long compared to the correlation time $\tau_c=1$.

Figure 11 explores more carefully the high-frequency (short-time scale) part of the Ornstein-Uhlenbeck process. The curves are rather similar to those already calculated for the Wiener process in Fig. 6(a) except for the shift in time scale. This suggests that the high-frequency part of the time series is accurately self-affine for those frequencies for which the power spectrum is approximately a power law. We conjecture that this conclusion holds more generally, since the smooth part of the flow is effectively constant on such short time scales.

IV. CONCLUSIONS

In this paper, we have analyzed numerically the self-affine properties of time series with an imposed power-law power spectrum. Extending the results of earlier investigators [14–17], we have studied the consequences of different choices of phases by varying their correlation times, their probability distributions, and their fractal dimensions. Using two criteria for self-affinity, a length-based fractal dimension of the graph [14,17] and a new test proposed by us [Eq. (17)], we found that time series are accurately self-affine for the special case $\alpha=2$, provided the phases are approximately δ-function correlated. For values $\alpha\neq 2$, time series were much less accurately self-affine, e.g., there were systematic deviations in the local slope from the expected straight line, and the average local slope did not agree with the theoretical values.

We conclude that a power-law spectrum is generally not sufficient to give self-affine scaling. While not important for graphics applications [19], this observation has useful implications for the analysis of empirical physics or economics data, for which power-law spectra are often observed. Our results show quantitatively the quality of

scaling curves for different values of α, and are summarized in Figs. 5 and 9.

A second important result in this paper was the introduction of a method for studying self-affinity in time series, based on the moments of probability distributions Eq. (17). We have shown that this test is more subtle than other tests discussed in Sec. II C, especially tests based on the fractal dimension of the graph. Fractal dimensions give similar results for all phases that are δ-function correlated, while the test based on moments distinguishes between phases that have uniform and nonuniform probability distributions. Results in Sec. III C show that our method is also sensitive to time scales in the problem, and so complements the test of studying the collapse of different probability distributions to a single curve [3]. It would be interesting at this point to apply this test to various data [6,3,4] and to compare the results with earlier studies.

Several important theoretical problems remain. One is to explain the slow (logarithmic?) convergence of time series with power-law power spectra towards self-affine behavior [17] for $\alpha \neq 2$ as the length of the time series is increased. Does a statistical limit exist that is independent of the properties of the phase distribution? A second problem is to find more accurate algorithms for self-affine time series than those generated by Eq. (4) in the random-phase approximation. It will probably be fruitful to return to Mandelbrot's more direct approximation of fractional Brownian motion [36,9] and to analyze the resulting time series using the methods proposed herein. A final problem is to find physical mechanisms that generate the approximately self-affine time series observed in fluid transport [3] and in granular flow [4].

ACKNOWLEDGMENTS

We would like to thank William Baxter, Robert Behringer, James Theiler, and Robert Wolpert for useful discussions. This work was supported by a summer research grant of the Business Foundation of North Carolina, by National Science Foundation (NSF) Grants No. ASC-8820327, and No. DMS-8804592, and by an allotment of CRAY CPU time at the North Carolina Supercomputing Center.

*Electronic address: ugreis@unc.bitnet.
†Electronic address: hsg@cs.duke.edu.

[1] L. F. Burlaga and L. W. Klein, J. Geophys. Res. **91**, 347 (1986).
[2] A. R. Osborne and A. D. Kirwan, Physica D **23**, 75 (1986).
[3] R. Ramshankar, D. Berlin, and J. P. Gollub, Phys. Fluids A **2**, 1955 (1990).
[4] G. William Baxter, Ph.D. thesis, Duke University, Department of Physics, 1990.
[5] C. W. J. Granger, Econometrica **34**, 150 (1966).
[6] Wentian Li, Int. J. Bifurcation Chaos (to be published).
[7] H. Tennekes and J. L. Lumley, *A First Course in Turbulence* (MIT, Cambridge, 1972).
[8] B. B. Mandelbrot, *The Fractal Geometry of Nature* (Freeman, New York, 1983).
[9] Jens Feder, *Fractals* (Plenum, New York, 1988).
[10] S. James Taylor, Math. Proc. Cambridge Philos. Soc. **100**, 383 (1986).
[11] J. B. Carlin and A. P. Dempster, J. Am. Stat. Association **84**, 6 (1989).
[12] Philip Mirowski, South. Econ. J. **57**, 289 (1990).
[13] S. Panchev, *Random Functions and Turbulence* (Pergamon, Oxford, 1971).
[14] T. Higuchi, Physica D **31**, 277 (1988).
[15] Christopher G. Fox, Pure Appl. Geophys. **131**, 211 (1989).
[16] A. R. Osborne and A. Provenzale, Physica D **35**, 357 (1989).
[17] T. Higuchi, Physica D **46**, 254 (1990).
[18] S. O. Rice, in *Noise and Stochastic Processes,* edited by Nelson Wax (Dover, New York, 1954), pp. 133–294.
[19] *The Science of Fractal Images,* edited by Heinz-Otto Peitgen and Dietmar Saupe (Springer-Verlag, New York, 1988).
[20] Pierre Bergé, Yves Pomeau, and Christian Vidal, *Order Within Chaos* (Wiley, New York, 1984).
[21] W. H. Press, B. P. Flannery, S. A. Teukolsky, and W. T. Vetterling, *Numerical Recipes in C* (Cambridge University, New York, 1988).
[22] P. Grassberger and I. Procaccia, Physics D **9**, 189 (1983).
[23] James Theiler, Phys. Rev. A **36**, 4456 (1987).
[24] A. J. Lichtenberg and M. A. Lieberman, *Regular and Stochastic Motion,* Vol. 38 of *Applied Mathematical Sciences* (Springer-Verlag, New York, 1983).
[25] N. Wax, *Noise and Stochastic Processes* (Dover, New York, 1954).
[26] B. B. Mandelbrot, Phys. Scripta **32**, 257 (1985).
[27] Richard F. Voss, Physica D **38**, 362 (1989).
[28] P. Grassberger, Phys. Lett. **107A**, 101 (1985).
[29] J.-P. Eckmann and D. Ruelle, Rev. Mod. Phys. **57**, 617 (1985).
[30] James Theiler, Phys. Rev. A **34**, 2427 (1986).
[31] James Theiler, Phys. Lett. A **155**, 480 (1991).
[32] H. S. Greenside, G. Ahlers, P. C. Hohenberg, and R. W. Walden, Physica D **5**, 322 (1982).
[33] D. Sigeti and W. Horsthemke, Phys. Rev. A **35**, 2276 (1987).
[34] Uriel Frisch and Rudolf Morf, Phys. Rev. A **23**, 2673 (1981).
[35] Paul Manneville, Phys. Lett. A **84**, 129 (1981).
[36] B. B. Mandelbrot, Water Resour. Res. **7**, 543 (1971).
[37] H. S. Greenside and E. Helfand, Bell Syst. Tech. J. **60**, 1927 (1981).